Steplike Magnetization in a Spin-Chain System: $Ca_3Co_2O_6$

Yuri B. Kudasov*

Institut de Physique et Chimie des Matériaux de Strasbourg, 67034, Strasbourg, France
and Russian Federal Nuclear Center - VNIIEF, Sarov, 607188, Russia

(Received 1 August 2005; published 19 January 2006)

Because of a ferromagnetic in-chain coupling between Co^{3+} ions at trigonal sites, Co_2O_6 chains are considered as large rigid spin moments. The antiferromagnetic Ising model on the triangular lattice is applied to describe an interchain ordering. An evolution of metastable states in a sweeping magnetic field is investigated by the single-flip technique. At the first approximation two steps in the magnetization curve and a plateau at $1/3$ of the saturation magnetization are found. Four steps in magnetization are determined in high-order approximations in agreement with experimental results.

DOI: 10.1103/PhysRevLett.96.027212 PACS numbers: 75.25.+z, 75.30.Kz, 75.50.Ee

Among other spin-chain compounds, $Ca_3Co_2O_6$ has recently drawn considerable attention to their unique magnetic behavior [1–5]. The most intriguing feature observed in $Ca_3Co_2O_6$ is a steplike shape of the magnetization curve [2,3,5]. The number of the steps in the curve depends strongly on a sweep rate of the external magnetic field and temperature [2,3,5]. Two steps become apparent in the temperature range from 12 to 24 K [5]. The first step takes place at zero magnetic field. Then the magnetic moment remains constant at about $1/3$ of the full magnetization up to the magnetic field of 3.6 T where the second step occurs to the fully magnetized FM state. At least four steps that are equidistant on the magnetic field are clearly visible below 10 K at a very low sweep rate. They are accompanied by a sizeable hysteresis. Similar phenomena were observed in other spin-chain compounds, e.g., Ca_3CoRhO_6 [6,7].

The structure of $Ca_3Co_2O_6$ consists of Co_2O_6 chains running along the c axis. The Ca ions are situated between them. The chains are made up of alternating, face-sharing CoO_6 trigonal prisms and CoO_6 octahedra. The crystalline electric field splits the energy level of Co^{3+} ions into the high-spin ($S = 2$) and low-spin ($S = 0$) states. The Co^{3+} ions situated in the trigonal environment (CoI) are in the high-spin state and the octahedral Co sites (CoII) occurs in the low-spin state. In the last case the energy difference between the low-spin and high-spin states is very small and a tiny fraction of CoII sites is reported to be in the high-spin state. The crystalline electric field leads also to a very strong Ising-like anisotropy at the CoI sites. The chains form triangular lattice in the ab plane that is perpendicular to the chains. An in-chain exchange interaction between magnetic CoI ions through the octahedra with nonmagnetic CoII ions is ferromagnetic (FM). It causes the in-chain FM ordering of CoI ions at about 40 K. The interchain interaction is antiferromagnetic (AFM) and much weaker than the in-chain one. A partial AFM order of chains appears at 24 K. A weak feature concerned most probably with a transition in a new interchain order was also observed at around 12 K. This scenario of magnetic interactions in $Ca_3Co_2O_6$ is consistent with results of x-ray photoemission spectroscopy [8], neutron scattering [9], magnetization and specific heat measurements [1–5,10], nuclear magnetic resonance [11], and theoretical calculations of indirect interactions between CoI sites [12].

The model presented in Ref. [2] deals with an in-chain structure of $Ca_3Co_2O_6$ and magnetization dynamics explained in terms of the quantum tunneling. In this Letter, we develop a new model for a description of the steplike magnetization in $Ca_3Co_2O_6$ at low temperatures, shifting the stress on the interchain magnetic order. The strong FM in-chain coupling makes it possible to consider a Ca_2O_6 chain as a large rigid spin formed by CoI ions. There are only two projections of the chain spin onto the c axis due to the strong Ising-like anisotropy. Including the AFM coupling between the nearest-neighbor chain spins we arrive to the Ising Hamiltonian on the triangular lattice

$$H = J\sum_{\langle ij\rangle}\sigma_i^z\sigma_j^z - B\sum_i\sigma_i^z, \tag{1}$$

where $\sigma_i^z = \pm 1$ is the c-axis projection of the ith chain spin, $J > 0$ is the parameter of the AFM interchain coupling, B is the magnetic field, and $\langle ij\rangle$ denotes the summation over all the nearest-neighbor pairs on the triangular lattice.

The strong dependence of the magnetization curve shape on the magnetic field sweep rate and temperature shows that the state of the system of the chain spins in the magnetic field is far from equilibrium. At the low sweep rate the system is rather in a metastable state than in the ground state. It is convenient to formulate necessary conditions of the metastability of the system in the following form:

$$\sigma_i^z h_i \le 0, \tag{2}$$

where

$$h_i = J\sum_{j(i)}\sigma_j^z - B$$

is the effective field for the ith chain and $j(i)$ denotes summation over the nearest neighbors of the ith chain. We have used the unstrict inequality in Eq. (2) keeping in mind a strong degeneracy of partially ordered AFM arrangements on the triangular lattice. A transition from one metastable state to another occurs through exited states. We obtain $\sigma_i^z h_i > 0$ at least for one chain in a exited state by definition. Let $\Delta E_i = 2\sigma_i^z h_i > 0$ be the excitation energy per CoI site of the ith chain. It follows from this that the probability of an exited chain at low temperature T is extremely small $\propto \exp(-N\Delta E_i/T)$ since the number of CoI sites in the chain (N) is considered to be large. That is why we should investigate an evolution of metastable states in the slowly sweeping external magnetic field assuming $T = 0$ quench.

We perform the investigation of the evolution of the system using the single-flip technique that was applied earlier to nonequilibrium dynamics of the AFM Ising model on the triangular lattice [13]. In the terms of the effective field, the spin-flip probability A is taken in the following form:

$$A = \begin{cases} 0 & \text{if } \sigma_i^z h_i < 0, \\ 1 & \text{if } \sigma_i^z h_i \geq 0. \end{cases} \tag{3}$$

In contrast to Ref. [13] where the spin-flip technique was applied to numerical Monte Carlo simulations, we investigate the evolution analytically. If a state under consideration is degenerate and different sequences of spin flips lead to different final states, one should take into account each possible sequence with equal probabilities. This assumption can be proven rigorously by Bogolubov's quasiaverage technique. That is, a small auxiliary random field should be added to the Hamiltonian (1) in order to lift the degeneracy. After that we take an average over a manifold of the auxiliary fields restoring equivalence of different chains and, then, let the amplitude of the auxiliary fields goes to zero. This approach is equivalent to the Monte Carlo technique in the limit of the large number of samples.

We take the ground state of the triangular lattice as an initial state of the chain lattice at $B = 0$. The ground state of triangular lattice at $B = 0$ is strongly degenerate and it is impossible to represent it in an explicit form [14]. On the other hand, we can produce a set of approximations for the ground state. Since the entropy density for the ground state was calculated exactly by Wannier [14] as

$$S = \frac{2}{\pi} \int_0^{\frac{\pi}{3}} \ln(2\cos\omega) d\omega \approx 0.3231, \tag{4}$$

we are able to compare the entropy density of the approximated state to the exact value in order to control the precision of our approximation. Previously, Maignan *et al.* [5] performed a qualitative analysis of the magnetization curve starting with an initial state that consisted of alternating rows of spin-up and spin-down chains. The energy of such an arrangement equals the ground state energy but its statistical weight goes to zero in the limit of the infinite lattice. Therefore, arrangements of this type should be discarded [14].

The first approximation to the ground state of the AFM Ising model on the triangular lattice is the honeycomb structure shown in Fig. 1. Two thirds of the total number of the chain spins are ordered in the AFM honeycomb structure, whereas other chain spins placed in the centers of hexagons have arbitrary projections of chain spins onto the c axis. The entropy density of the first approximation equals $S_1 = (1/3)\ln 2 \approx 0.231$. An arbitrary small external magnetic field lifts degeneracy of chain spins in the centers of hexagons orienting them along the magnetic field ($\sigma_i^z = 1$). We consider that the spin-up chains (the black circles) are directed parallel to the magnetic field. The gray circles become black in Fig. 1. This causes a step at $B = 0$ with the height of $1/3$ where the full magnetization is taken as unity. Then, one third of the spin chains remain spin-down or antiparallel to the field. Since they are surrounded by 6 spin-up chains this configuration is stable up to the critical magnetic field $B_C = 6J$ where a transition to the fully-polarized FM state takes place. The magnetization curve for the first approximation is shown in Fig. 2. It should be noticed that this curve is in an excellent agreement with the experimental data at the intermediate temperatures [1–3,5].

We can improve the approximation used above including tripod configurations [14]. Since the chains placed in the centers of hexagons have arbitrary projections of the spin onto the c axis, it occurs that three of them neighboring with the same chain of the honeycomb sublattice are in the same state. Then the configuration shown in Fig. 3 can appear. The chain spin in the center of the tripod belongs to the honeycomb sublattice but, nevertheless, it can have an arbitrary c projection of the chain spin. These states increase the entropy density up to $S = (5/12)\ln 2 \approx 0.289$ [14] and involve various types of configurations: isolated tripods and connected tripods. It is convenient to consider them separately. After straightforward calculations we obtain the probability of an isolated tripod

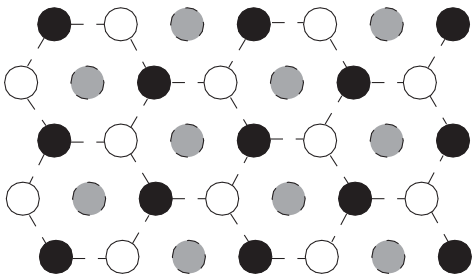

FIG. 1. The honeycomb magnetic structure. The black and white circles are spin-up and spin-down states, respectively; the gray circles can be either spin-up or spin-down states.

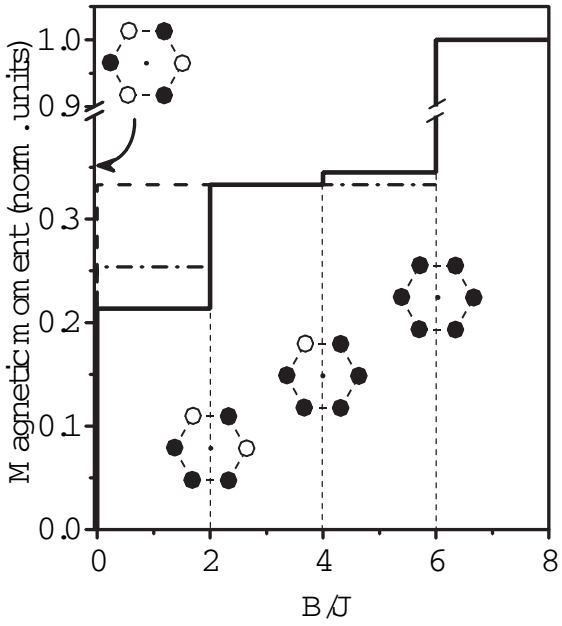

FIG. 2. The magnetic moment as a function of the dimensionless magnetic field B/J. The dash, dash-dot, and solid lines are the results of the first, second, and fourth approximations, correspondingly. The four nearest-neighbor configurations producing the critical spin-flip fields are shown. Note the break in the vertical axis.

$$P_2 = (1/12)(1 - 1/2^3 - 1/2^4 - 1/2^5)^3 \approx 0.0397. \quad (5)$$

We include this type of configuration in the second approximation for the initial state. The entropy density of the second approximation is $S_2 \approx 0.259$. Applying the external magnetic field we again obtain a step at the zero magnetic field but the chain spins in the centers of hexagons sharing joint corners with the tripod center remain in the spin-down state because they are surrounded by 4 spin-up and 2 spin-down nearest neighbors. The height of the step $[\Delta M(B/J)]$ can be expressed through probability of the isolated-tripod configuration as $\Delta M(0) = (1/3) - 2P_2$. The spin chains in the centers of the tripod hexagons flip at the new critical magnetic field $B_C = 2J$. While the magnetic fields increases further, the curve occurs at the $1/3$ plateau and coincides with the curve obtained in the first approximation (see Fig. 2).

The third approximation is to include configurations with isolated pairs of connected tripods. These configurations change the heights of the steps but give no new features in the magnetization curve. The probability of the pair of isolated tripod is $P_3 \approx 0.010$. The entropy density increases up to $S_3 \approx 0.273$.

An isolated configuration of three tripods connected as a star is taken into account in the framework of the fourth approximation (see Fig. 4). The probability of this configuration is $P_4 \approx 0.0035$ and the entropy density in the fourth approximation is $S_4 \approx 0.280$. The key feature of this configuration is that there are chain spins that are surrounded by 5 spin-up and one spin-down nearest neighbors. These chain spins remain stable up to the new critical magnetic field $B_C = 4J$. To calculate the step in the magnetization curve we have to calculate a number of various sequences of spin flips. The final value of the step is $\Delta M(4) \approx 0.008$, which is significantly smaller than $\Delta M(2) \approx 0.12$.

There is a variety of more complex configurations than the tripod. However, it should be mentioned that further approximations should change the heights of the steps but they cannot cause new features in the magnetization curve. As it follows from Eq. (2) there exist only four critical magnetic fields related to the four configurations of the nearest neighbors shown in Fig. 2.

The magnetization curve obtained in the fourth approximation reproduces the key features of the experimental data at the very low sweep rate, namely, the four equidistant steps in the magnetization curve. In contrast with our results, the third step in the experimental curve is much larger than the second one. This quantitative discrepancy can be eliminated in higher order approximations that can be investigated both analytically, by the technique used in this Letter, or numerically, applying Monte Carlo simula-

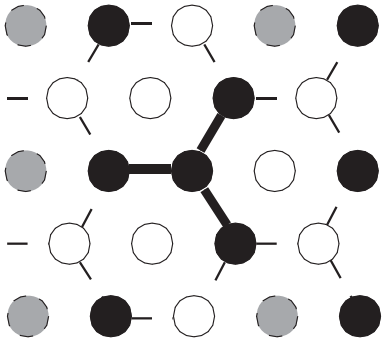

FIG. 3. An arrangement containing the tripod configuration. The tripod is shown in the solid line. The three white circles close to the center of the tripod have 4 spin-up (the black circles) and 2 spin-down (the white circles) nearest neighbors.

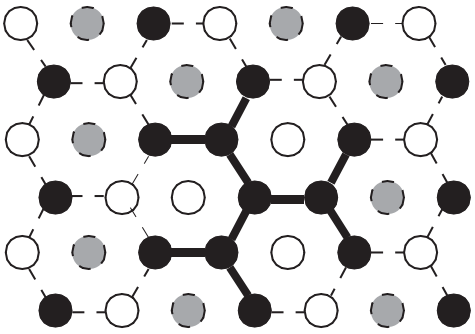

FIG. 4. Three tripods connected in the star arrangement. Three white circles close to the center of the star are surrounded by 5 spin-up and 1 spin-down nearest neighbors.

tion [13]. Approximations of higher orders are of importance for quantitative calculations of the magnetization curve because the calculation convergence for the magnetic moment is slower than that for the configuration probability.

Few questions on the magnetization of $Ca_3Co_2O_6$ are still unclear. There were observed weak smeared features in the experimental curve at high magnetic fields above the last step. They can stem from the small fraction of CoII sites that are the high-spin state, because they increase the chain spin and cause higher critical fields. The sizeable hysteresis also draws attention in the experimental curve. It depends drastically on the temperature and the magnetic field sweep rate. It should be mentioned that while the magnetic field sweeps down and crosses the highest critical field $B_C = 6J$ the chain spins flip down at random and the system occurs in a new state that is different from that at the sweeping-up process.

The model developed above can be easily generalized to the magnetization dynamics. The spin-flip process of an Ising chain consists of a consequence of transitions over exited states. That is why the probability of the spin flip per a unit of time is proportional to the factor of $\exp(-\frac{\Delta}{T})$ where Δ is the activation energy. Thus, one can numerically investigate the dependence of the magnetization curve on the temperature and the magnetic field sweep rate applying the spin-flip technique [13].

In conclusion, we have developed a new model for the steplike magnetization of $Ca_3Co_2O_6$ spin-chain compound. It can be applied also to other spin-chain compounds with the triangular lattice of chains, e.g., Ca_3CoRhO_6. Because of the in-chain FM coupling between Co^{3+} ions at trigonal sites, Co_2O_6 chains are considered at low temperatures as large rigid spins with the strong Ising-like anisotropy. The AFM Ising model on the triangular lattice is applied to the system of rigid FM-ordered chains. The crucial point of the model is the supposition that the system is out of equilibrium, because the dependence of the magnetic moment on the magnetic field in the ground state of the AFM Ising model on the triangular lattice is smooth with the exception of the step at the zero magnetic field [15]. For the honeycomb AFM structure two steps were found in the theoretical magnetization curve in excellent agreement with experimental data at the intermediate temperatures. At higher approximations four equidistant steps were determined in accordance with experimental curves at the low temperatures and very low magnetic field sweep rate. The results obtained in this Letter and the model of Ref. [2] can be regarded as two limiting cases. The first deals with the nonequilibrium interchain ordering assuming the chain spins to be rigid. An in-chain fragmentation and the quantum tunneling of the magnetic moment of the fragments are investigated in the second case, totally neglecting the interchain ordering.

I am grateful to C. Demangeat and M. Drillon for fruitful discussions and hospitality during my stay at Institut de Physique et Chimie des Matériaux de Strasbourg en Unité mixte de recherche. This study was partially supported by the INTAS grant (03-51-4778) ''Hierarchy of scales in magnetic nanostructures.''

*Electronic address: kudasov@ntc.vniief.ru

[1] V. Hardy, D. Flahaut, M. R. Lees, and O. A. Petrenko, Phys. Rev. B **70**, 214439 (2004).
[2] A. Maignan, V. Hardy, S. Hebert, M. Drillon, M. R. Lees, O. Petrenko, D. M. K. Paul, and D. Khomskii, J. Mater. Chem. **14**, 1231 (2004).
[3] V. Hardy, M. R. Lees, O. A. Petrenko, D. M. K. Paul, D. Flahaut, S. Hebert, and A. Maignan, Phys. Rev. B **70**, 064424 (2004).
[4] V. Hardy, S. Lambert, M. R. Lees, and D. M. K. Paul, Phys. Rev. B **68**, 014424 (2003).
[5] A. Maignan, C. Michel, A. C. Masset, C. Martin, and B. Raveau, Eur. Phys. J. B **15**, 657 (2000).
[6] S. Nijtaka, K. Yoshimura, K. Kosuge, M. Nishi, and K. Kakurai, Phys. Rev. Lett. **87**, 177202 (2001).
[7] S. Nijtaka, H. Kageyama, K. Yoshimura, K. Kosuge, S. Kawano, N. Aso, A. Mitsuda, H. Mitamura, and T. Goto, Phys. Rev. Lett. **87**, 177202 (2001).
[8] K. Takubo, T. Mizokawa, S. Hirata, J.-Y. Son, A. Fujimori, D. Towal, D. D. Sarma, S. Rayaprol, and E.-V. Sampathkumaran, Phys. Rev. B **71**, 073406 (2005).
[9] S. Aasland, H. Fjellvag, and B. Hauback, Solid State Commun. **101**, 187 (1997).
[10] B. Martinez, V. Laukhin, M. Hernando, J. Fontcuberta, M. Parras, and J. M. Gonzalez-Calbet, Phys. Rev. B **64**, 012417 (2001).
[11] E.-V. Sampathkumaran, N. Fujiwara, S. Rayaprol, P. K. Madhu, and Y. Uwatoko, Phys. Rev. B **70**, 014437 (2004).
[12] R. Fresard, C. Laschinger, T. Kopp, and V. Eyert, Phys. Rev. B **69**, 140405 (2004).
[13] E. Kim, B. Kim, and S. J. Lee, Phys. Rev. E **68**, 066127 (2003).
[14] G. H. Wannier, Phys. Rev. **79**, 357 (1950).
[15] D. C. Mattis, *The Theory of Magnetism II* (Springer-Verlag, Berlin, 1985).